Differential Optical Sensing through Coupled Micro Ring Resonators

Ali Emre Kaplan, Geatano Bellanca

Department of Engineering
University of Ferrara
Ferrara, Italy
e-mails: aliemre.kaplan@unife.it, gaetano.bellanca@unife.it

Paolo Bassi

Department of Electrical, Electronic and Information Engineering
University of Bologna
Bologna, Italy
e-mail: paolo.bassi@unibo.it,

***Abstract*—We theoretically investigate the performance of a double micro ring resonator for integrated optical sensing applications. The transmission characteristics of the proposed device can be driven in two distinct operations by controlling the difference of the round-trip phase shifts of the coupled resonators. The enhancement of the limit of detection by a factor of 5.6 compared to a single micro ring based sensor is demonstrated. Beside the fact that the single and double ring based schemes have the same spectral wavelength sensitivity of 918 nm per refractive index unit, the latter scheme also supports the intensity interrogation which can be used for on-chip thermal noise compensation via integrated micro heaters.**

Keywords*–*Micro ring resonators; Optical sensing; Integrated photonic circuits.

I. Introduction

Integration of microfluidics with Photonic Integrated Circuits (PIC) promotes new emerging biosensing technologies. Especially Silicon based on-chip sensors draw an intense interest thanks to their compactness, cost effectiveness and Complementary Metal-Oxide Semiconductor (CMOS) compatible properties. So far, various types of on-chip Si PICs, such as Micro Ring Resonator (MRR), Mach–Zehnder interferometer, photonic crystal and Bragg grating have been investigated for label-free detection [1] and, among them, MRR based sensors provide higher sensitivity and denser integration [2]. A comprehensive review paper about Silicon MRR based biosensors can be found in [3]. The add-drop configuration of MRR allows a sensing application that measures the resonance wavelength shift according to up cladding index change induced by microfluids [4]. Figure 1 illustrates a typical working principle of a ring based sensing scheme. A suitable measurement setup for such devices consists of a tunable laser source that provides the incoming light and a spectrometer to measure the spectral shift of resonance wavelengths after binding.

The characterization wavelength interrogation is based on the extraction of refractive index change information via resonant wavelength shifts induced by the interaction of fluids and the evanescent field of a resonant cavity. The resonance wavelength of a single ring is defined as

$$m \cdot \lambda_{res} = n_{eff} L \tag{1}$$

where L is the circumference of the ring, n_{eff} is the effective refractive index of the resonant mode and m is an integer, and a modification of n_{eff} results in a variation of λ_{res}. The amount of the wavelength shift depends on how much flowing analyte alters the effective refractive index and it can

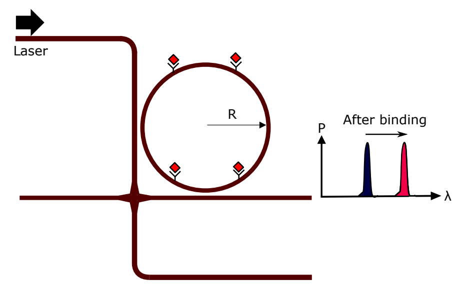

Figure 1. Schematic of a conventional micro ring resonator based biosensor.

be formulated as [5]

$$\Delta\lambda = \frac{\Delta n_{clad} \lambda_{res}}{n_g} \tag{2}$$

where n_g is the group index of the guided mode and Δn_{clad} is the refractive index change of the cladding induced by the interaction of the fluids and the ring resonator. This interaction can occur either by analyte binding or concentration change of substances and the types of sensing are then called label-free and bulk sensing, respectively. The MRR with high quality factor, or Q-factor, is desirable for enhanced detection limit of sensing applications. However, environmental and microfluidics induced thermal perturbations must be considered since such spurious effects may significantly affect the spectral wavelength shift at higher Q-factor. Previously, a sensing scheme based on cascaded MRRs has been investigated using shared flow channel above the reference and sensing rings where two solutions flow independently [6]. However, it was found difficult to control precisely the temperature and pressure of each solution. Another approach uses two frequency locked laser sources for imprinting the temperature difference of the rings in radio-frequency domain and achieves the state of the art sensitivity in the order of 10^{-8} RIU (Refractive Index Unit) [7] but still this method suffers from lack of thermal equilibrium of the sensor and requires more than one laser source. The previously reported differential sensing platforms with thermal compensation perform only wavelength interrogation. Here, we propose an alternative scheme based on a double ring structure that is able to also support the intensity interrogation that can help to eliminate the need of external thermal stabilization systems and a reference fluid flow. In Figure 2, the working principle of the proposed device

 ISBN: 978-1-61208-749-8

is illustrated. Two micro rings with the radius R_1 and R_2 are indirectly coupled via a central bus waveguide. When the two rings are synchronized ($\theta_1 = \theta_2$), both resonators share the same resonance wavelength and thanks to the common light path, which is the vertical waveguide section, the switched wavelength propagates back to the input port, as shown in Figure 2a. In this case, the through port in the middle and the upper and bottom drop ports have transmission dips. In the second operational regime, each ring switches its own resonance wavelengths to the upper and bottom drop ports, as a result of different round-trip phase shifts ($\theta_1 \neq \theta_2$). The through port has, therefore, two transmission dips where the resonances appear and the transmitted powers at the drop ports increase (see Figure 2b). The phase shift difference of the two paths can be determined by different radius of the two rings or by effective index detuning of the one of two ring waveguides through, e.g., thermo-optic effect, if the resonators have equal radii.

In our theoretical work, we assume that the rings are identical and the induced effective index change occurs in one of the rings, while the other ring is being used as the reference one. Since the overall output transmissions depend only on the phase difference, we refer to this scheme as a differential sensing scheme.

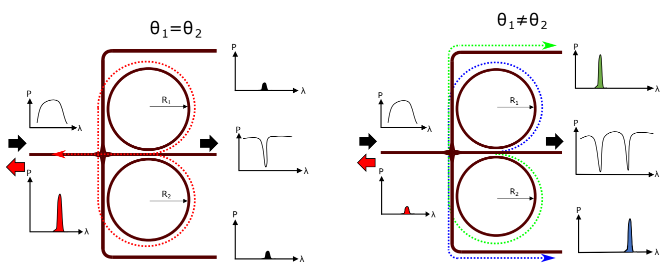

(a) (b)

Figure 2. Working principle of the coupled ring sensing scheme: synchronous phase shift (a) and asynchronous (b) after binding.

In this work, we will theoretically discuss the performance of the proposed sensing scheme in terms of sensitivity, Limit of Detection (LOD) and thermal compensation by comparing the proposed configuration to the conventional single ring results analyzed using the same design parameters, such as coupling strength of the vertical and horizontal coupling sections, waveguide geometry and radius. The paper is organized as follows. In Section 2, we introduce sensor parameters, sensitivity and limit of detection. Also, we show the effect of phase synchronization on the transmission behavior of the sensor. Section 3 provides the results of both wavelength and intensity interrogations and compare the results of the differential sensing to those obtained from the single ring configuration. Finally, we discuss the better performance attained by using differential sensing for practical issues, such as the sensor calibration and thermal compensation.

II. Transmission Characteristics of the Proposed Sensing Scheme

We analytically study both structures based on the Transfer Matrix Method obtained from coupling relationships of the resonators in the two port and three port coupler sections [8]–[10]. The design parameters such as radii of the rings and coupling ratios of the horizontal and vertical couplers are inserted in the transfer matrices. The effective refractive index n_{eff} of the Transverse Electric (TE) mode propagating of the Silicon-On-Insulator (SOI) waveguide (480x220 nm), are obtained through the Finite Element Method (FEM) simulations [11]. In our scenario, the bottom ring is considered as a reference and its round trip phase shift (θ_2) can be detuned by, for example, micro integrated heaters. Instead, the phase shift of the upper sensor ring (θ_1) changes due to the presence of the specimen. Assuming that $R_1 = R_2$, then round trip phase shifts for sensor and reference rings are defined as $\theta_1 = n_{eff_1} \cdot L$ and $\theta_2 = n_{eff_2} \cdot L$, respectively. A special case occurs when the rings have the same phase shift as shown in Figure 3a. The reflected wavelength reaches its maximum near critical coupling where a high extinction ratio is present for the through port along with weak drop port transmissions. When the effective index of the sensor ring is changed due to the binding of analytes on the cladding, the reference signal (green curve) remains at the same wavelength, while the sensing wavelength (blue curve) experiences red shift, as shown in Figure 3b. In addition, the reflection power decreases dramatically.

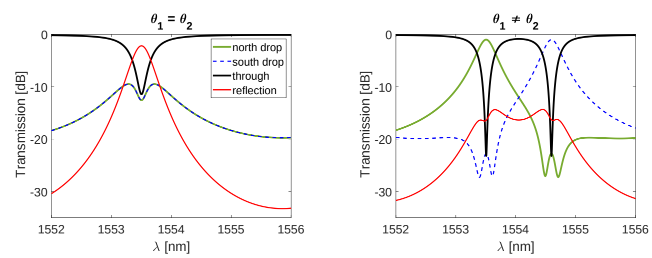

(a) (b)

Figure 3. Transmitted powers of through port (black), upper and bottom drop ports (green and blue) and back reflection (red) in initial condition (a) and sensing operation (b).

In order to evaluate pros and cons of the presented device over the single ring scenario, we first need to calculate its sensitivity using the following description [3]:

$$S = \frac{\Delta\lambda}{\Delta n_{clad}} \tag{3}$$

As we analyze the device theoretically, it is convenient to use the Δn_{eff} instead of the Δn_{clad} because the rings are identical in both single and double ring schemes. The minimum detectable change of the n_{neff} determines the LOD which corresponds also to the minimum wavelength shift $\Delta\lambda$. Since this sensing scheme requires a spectrum analysis, minimum detection depends on the setup. To eliminate setup dependency of the measurements, an intrinsic LOD ($iLOD$) can be defined as [3]:

$$iLOD = \frac{FWHM}{S} \tag{4}$$

meaning that the Full Width Half Maximum (FWHM) of the resonance peak is the lower limit of the wavelength shift needed to distinguish two successive wavelengths. S and $iLOD$ are used as the test parameters to investigate the performance of the device.

III. Performance comparison of single and coupled double ring sensors

An example of wavelength shifting at the drop ports obtained from n_{eff} detuning is illustrated in Fig 4. Both rings have the same radius of $20\mu m$ and the coupling ratio is fixed at $K = 0.1$ for both single and double ring configurations. The green curves and the blue curves in Figure 4a represent reference and sensing signals of the double ring sensor, respectively. In the double ring scheme, the sensing signal exhibits a red-shift and an intensity increase, while the reference signal intensity increases by maintaining the fixed wavelength. On the other hand, the single ring sensor (see Figure 4b) has only wavelength shift with negligible peak intensity variations. Thus, the double ring configuration also allows to analyze intensity interrogation in addition to wavelength interrogation.

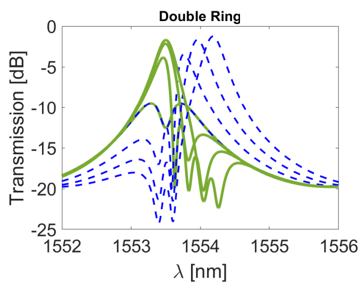

(a)

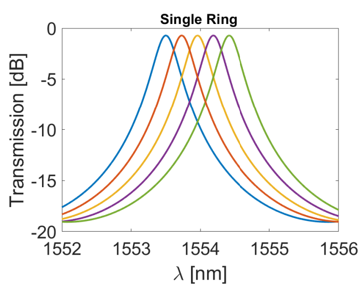

(b)

Figure 4. Wavelength shifts induced by the change effective refractive index of the drop ports of the double ring (a) and the single ring (b) configurations.

The comparison of the two schemes is shown in Figure 5. According to the Δn_{eff}, the wavelength shifts $\Delta\lambda$ (red lines) linearly increase in both devices. However, the peak intensity variation ΔP (blue curves) is available only for the double ring sensor and it shows a rapid increase for a small range of Δn_{eff}, as shown in Figure 5a. On the contrary, the single ring sensor has a very small change in peak intensities so the ΔP remains almost constant, as shown in Figure 5b. Table I summarizes the calculated sensing parameters. The wavelength shift sensitivity $S_{\Delta\lambda}$ nm/RIU (RIU:Refractive Index Unit) is calculated from the slopes of the $\Delta\lambda$ and, since both devices have identical rings, $S_{\Delta\lambda}$ is found to be the same (918 nm/RIU). As opposed to the single ring case, the minimum resonance intensity sensitivity of 515 dB/RIU within the range $\Delta n_{eff} = 0.001$ of the double ring sensor demonstrates that it is possible to achieve intensity interrogation for very accurate sensing performance in a small Δn_{eff} span. The $S_{\Delta P}$ increases as the index change span decreases. The most significant difference of the sensors appears for the limit of detection. The resonance line width determines the $iLOD$ such that it ensures at least 3 dB bandwidth separation of two successive resonances. We found that the coupled double ring sensor requires smaller effective refractive index change to meet $iLOD$ condition than single ring does and the detection limit of the double ring is found to be enhanced by a factor of 5.6 at the price of increased insertion loss of the sensor.

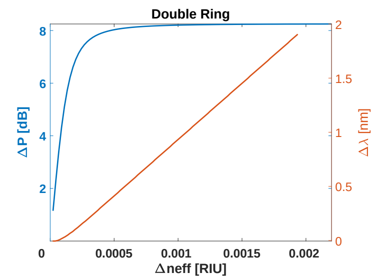

(a)

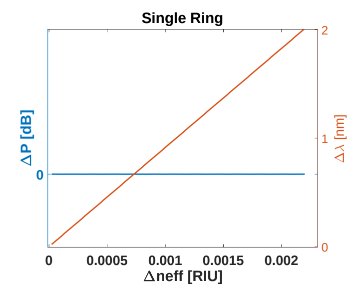

(b)

Figure 5. Comparison of ΔP (blue curve) and $\Delta\lambda$ (red curve) with respect to the induced Δn_{eff} for coupled double ring (a) and single ring (b) sensing schemes.

TABLE I. Calculated sensor parameters: sensitivities for wavelength $S_{\Delta\lambda}$ and intensity $S_{\Delta P}$ interrogations and detection limits.

	$S_{\Delta\lambda}[nm/RIU]$	$S_{\Delta P}[dB/RIU]$	$iLOD[RIU]$
Single Ring	918	0.6	$2.47 \cdot 10^{-4}$
Double Ring	918	515	$0.44 \cdot 10^{-4}$

The limiting factor for the intensity sensing is based on the convergence of the ΔP curve. For instance, when Δn_{eff} is equivalent to around 0.8 nm wavelength shift, the change in the transmitted power becomes negligible. This effect can be noticed from Figure 4a where the green curves around the maximum transmission are very close to each other. However, minimum detectable intensity change is limited by the power measurement accuracy. The curve of ΔP shown in Figure 5a can give different values of $S_{\Delta P}$ depending on the minimum acceptable intensity interval; we fixed such value at 0.1 dB and considered that changes below this value are negligible. Therefore, the reported $S_{\Delta P}$ in Table I is the minimum sensitivity. The maximum intensity sensitivity can be achieved in smallest Δn_{eff} such that the power of peaks increases very rapidly and reaches very high sensitivity up to $4.5 \cdot 10^4$ dB/RIU within the value of $iLOD$. Furthermore, it is possible to enhance the intensity interrogation range by increasing the coupling ratio, as shown in Figure 6. Stronger coupling strength gives rise to smoother transitions over the x-axes. But, as a consequence of an increased coupling ratio, the FWHM rises and results in $iLOD$ impairment.

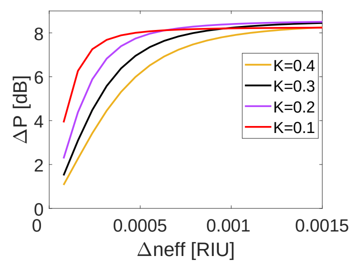

Figure 6. Effect of coupling ratio increments on the range of detectable Δn_{eff} in the intensity interrogation scheme.

One of the main noise sources for biosensors is thermal noise. Either environmental or resonator based self-induced thermal noise becomes critical for very highly sensitive sensors, hence the temperature of the sensor should be precisely controlled during the measurement. This adds another difficulty to realize reliable sensors. To overcome this issue, the proposed differential sensing scheme based on the coupled resonators can in fact provide an alternative approach to compensate thermal noise effects by an initial calibration of the reference ring phase shift by searching the local maximum of reflection that guarantees single resonance wavelength. Once two coupled rings are synchronized, which implies $\theta_1 = \theta_2$, then the resulting $S_{\Delta\lambda}$ and $S_{\Delta P}$ can be disposed of the thermal noise. During the sensing process, it is possible to retrieve spurious wavelength shift by monitoring the reference resonance wavelength. The amount of wavelength shift gives the portion of resonance shift of the sensing wavelength caused by thermal noises.

IV. Conclusion

We proposed and theoretically studied a novel optical biosensing scheme based on differential sensing through the coupled micro ring resonators in SOI technology. The assessment of the sensitivity and limit of detection of the proposed device is done by comparing the results obtained from the conventional single ring sensor, having the same technology design parameters such as coupling ratio and radius. Sensitivity of the wavelength interrogation is found to be identical for each type of device, while the double ring sensor has enhanced limit of detection by a factor of 5.6 compared to the single ring sensor.

In addition, the presented device also supports intensity interrogation which is not the case for single ring if only the spectral measurement is considered. However, such interrogation is found to be possible only for a very small effective refractive index change. The way of increasing the range of a detectable index change is reported and possible resulting impairment on the limit of detection is described.

Thanks to the possibility of an initial calibration of the device by monitoring the back reflection, differential sensing scheme can eliminate environmental and self-induced thermal noises. Therefore, this scheme can provide on-chip thermal control by integrated micro resistors on the reference ring for realizing reliable integrated biosensors and cost effective measurements.

References

[1] E. Luan, H. Shoman, D. M. Ratner, K. C. Cheung, and L. Chrostowski, "Silicon photonic biosensors using label-free detection," Sensors, vol. 18, no. 10, 3519, 2018. [Online]. Available: https://www.mdpi.com/1424-8220/18/10/3519 [retrieved: September, 2019].

[2] G. A. Rodriguez, S. Hu, and S. M. Weiss, "Porous silicon ring resonator for compact, high sensitivity biosensing applications," Opt. Express, vol. 23, no. 6, 2015, pp. 7111–7119.

[3] P. Steglich, M. Hülsemann, B. Dietzel, and A. Mai, "Optical biosensors based on silicon-on-insulator ring resonators: A review," Molecules, vol. 24, no. 3, 519, 2019. [Online]. Available: https://www.mdpi.com/1420-3049/24/3/519 [retrieved: September, 2019].

[4] T. Taniguchi *et al.*, "Detection of antibody-antigen reaction by silicon nitride slot-ring biosensors using protein g," Optics Communications, vol. 365, 2016, pp. 16 – 23.

[5] T. Claes *et al.*, "Label-free biosensing with a slot-waveguide-based ring resonator in silicon on insulator," IEEE Photonics Journal, vol. 1, no. 3, Sep. 2009, pp. 197–204.

[6] D. Kim *et al.*, "On-chip integrated differential optical microring refractive index sensing platform based on a laminar flow scheme," Opt. Lett., vol. 40, no. 17, Sep 2015, pp. 4106–4109.

[7] L. Stern *et al.*, "Ultra-precise optical to radio frequency based chip-scale refractive index and temperature sensor," Optica, vol. 4, no. 1, Jan 2017, pp. 1–7.

[8] Chang-Min Kim and Young-Joon Im, "Switching operations of three-waveguide optical switches," IEEE Journal of Selected Topics in Quantum Electronics, vol. 6, no. 1, 2000, pp. 170–174.

[9] H. Kogelnik and R. Schmidt, "Switched directional couplers with alternating $\Delta\beta$," IEEE Journal of Quantum Electronics, vol. 12, no. 7, 1976, pp. 396 – 401.

[10] A. Yariv, "Universal relations for coupling of optical power between microresonators and dielectric waveguides," Electronics Letters, vol. 36, no. 4, 2000, pp. 321–322.

[11] COMSOL Multiphysics, https://www.comsol.com [retrieved: September, 2019].